Hidden antibiotic resistance fitness costs revealed by GWAS-based epistasis analysis.

Maho Yokoyama[1], Maisem Laabei[2], Emily Stevens[3], Leann Bacon[3], Kate Heesom[4], Sion Bayliss[1], Nicola Ooi[5], Alex J. O'Neill[5], Ewan Murray[6], Paul Williams[6], Anneke Lubben[7], Shaun Reeksting[7], Guillaume Meric[1], Ben Pascoe[1], Samuel K. Sheppard[1], Mario Recker[8], Laurence D. Hurst[1], and Ruth C. Massey[3]*

1: Milner Centre for Evolution, Dept. of Biology and Biochemistry, University of Bath, UK
2: Division of Medical Protein Chemistry, Department of Translational Medicine, Lund University, S20502, Malmö, Sweden
3: School of Cellular and Molecular Medicine, University of Bristol, UK.
4: University of Bristol Proteomics Facility, University of Bristol, UK.
5: Antimicrobial Research Centre, Faculty of Biological Sciences, University of Leeds, Leeds, LS2 9JT, UK
6: Centre for Biomolecular Sciences, School of Life Sciences, University of Nottingham, NG7 2RD, UK.
7: Chemical Characterisation and Analysis Facility, Faculty of Science, University of Bath, BA2 7AY, UK
8: Centre for Mathematics and the Environment, University of Exeter, Penryn Campus, Penryn TR10 9FE, UK

* for correspondence: ruth.massey@bristol.ac.uk

ABSTRACT

Understanding how multi-drug resistant pathogens evolve is key to identifying means of curtailing their further emergence and dissemination. Fitness costs imposed on bacteria by resistance mechanisms are believed to hamper their dissemination in an antibiotic free environment, however, some have been reported to have little or no cost, which suggests there are few barriers preventing their global spread. One such apparently cost-free resistance mechanism acquired by the major human pathogen *Staphylococcus aureus* is to the clinically important antibiotic mupirocin, which is mediated by mutation of the highly-conserved and essential isoleucyl-tRNA synthethase (*ileS*) gene. In Genome Wide Association Studies (GWAS) on two genetically and geographically distinct MRSA lineages we have found this mutation to be associated with changes in bacterial virulence, driven through epistatic interactions with other loci. Given the potential dual effect of this mutation on both antibiotic resistance and virulence we adopted a proteomic approach and observed pleiotropic effects. This analysis revealed that the activity of the secretory apparatus of the PSM family of cytolytic toxins, the Pmt system, is affected in the mupirocin resistant mutant, which explains why it is less toxic. As an energetically costly activity, this reduction in toxicity masks the fitness costs associated with this resistance mutation, a cost that becomes apparent when toxin production is required. Given the widespread use of this antibiotic, and that this resistance often results from a single nucleotide substitution in the *ileS* gene, these hidden fitness costs provide an explanation for why this resistance mechanism is not more prevalent. This work also demonstrates how population-based genomic analysis of virulence and antibiotic resistance can contribute to uncovering hidden features of the biology of microbial pathogens.

55 **INTRODUCTION**

56 Antibiotic resistance can evolve in many ways, and frequently incur a fitness cost to
57 the organism[1] which has to either mutate the target site of the antibiotic, acquire
58 and express a gene encoding an alternative non-susceptible version of the target
59 protein, or acquire and produce an efflux pump that removes the antibiotic before it
60 can attack its target[2]. As antibiotics are most commonly used for short and defined
61 periods of time, resistant bacteria are under selection to reduce these costs to avoid
62 displacement once treatment has finished. In many cases this is achieved through
63 compensatory mutations that allow many resistance mechanisms to be maintained
64 stably populations for long periods of time[3]. However, some antibiotic resistance
65 mechanisms have been reported to incur no detectable fitness costs[4,5,6], which
66 suggests there are no barriers to their widespread dissemination.

67 *Staphylococcus aureus* is an example of a major human pathogen[7] that has
68 become more challenging to treat due to the emergence of antibiotic resistance,
69 with Methicillin-Resistant *S. aureus* (MRSA) being the most notable example[8]. *S.*
70 *aureus* resides asymptomatically as part of the normal nasal flora of up to 50% of
71 humans[9], however, this is a significant risk factor for infection[10], to the extent that
72 carriers are often decolonised using antibiotics such as mupirocin prior to invasive
73 procedures such as surgery or dialysis[11]. Mupirocin is a polyketide antibiotic that is
74 applied as an ointment to eradicate nasal carriage of MRSA in patients at risk of
75 infection[12]. Such decolonisation has been reported to reduce *S. aureus* infections of
76 post-surgical wounds by 58%, of haemodialysis patients by 80% and of peritoneal
77 dialysis patients by 63%[13].

78 The molecular target for mupirocin is the bacterial isoleucyl-tRNA synthetase
79 (IleRS), which charges tRNAs with the amino acid isoleucine (Ile)[12]. By binding to this
80 enzyme the antibiotic halts protein synthesis, so inhibiting bacterial growth[14]. As a
81 consequence of the widespread use of mupirocin, resistance has emerged where the
82 bacteria have mutated the gene encoding IleRS, *ileS*, resulting in an amino acid
83 substitution (e.g. V588F, encoded by a G to T single nucleotide polymorphism (SNP)
84 at position 1,762 in the *ileS* gene (G1762T)) which alters the structure of the
85 protein's active site, but retains functionality and renders mupirocin less effective[15].
86 This confers a low to intermediate level of resistance to the antibiotic[16].

87 Alternatively, the bacteria acquire an alternative IleRS, encoded by a *mupA* or *mupB*
88 gene, on a plasmid, which confers a higher level of resistance[17,18]. The prevalence of
89 mupirocin resistance varies widely, with the highest rates associated with patient
90 groups repeatedly exposed to the antibiotic[19,20]. It has also been shown that in
91 countries such as New Zealand and Australia which have previously reported a high
92 prevalence of mupirocin resistance, when restrictions were put in place limiting the
93 use of this antibiotic, the prevalence of resistant strains significantly declined[20]. This
94 suggests that antibiotic exposure is required to maintain selection of this resistance
95 mechanism within a population, despite it being reported as incurring no fitness
96 cost.
97 The *ileS* gene is highly conserved across the thousands of sequenced *S.*
98 *aureus* isolates, and many failed attempts to inactivate it suggest its activity is
99 essential to the bacteria. It is therefore surprising that the mutation that confers
100 mupirocin resistance, by altering the structure of the encoded protein, does not
101 appear to affect fitness. Especially considering that the replacement of the valine
102 588 (V588) with phenylalanine, a much bulkier residue, is likely to fill and distort the
103 Rossman fold of the enzyme, which is responsible for ATP binding activity of this
104 enzyme[4,10]. However, in a recent genome wide association study (GWAS) on the
105 major hospital acquired MRSA clone, ST239, this mutation was significantly
106 associated with differences in the virulence of *S. aureus* isolates[21]. Its effect on toxin
107 secretion, a major aspect of *S. aureus* virulence, was believed to result from epistatic
108 interactions between *ileS* and other polymorphic loci. Upon analysis of a second
109 genetically and geographically distinct collection of clinical isolates of the USA300
110 lineage we detected this epistasis signal again, and here we characterise the effect
111 this mutation has on both toxin production and bacterial fitness.
112
113 **RESULTS and DISCUSSION**
114 **Epistasis between the mupirocin resistance conferring mutation in the *ileS* gene**
115 **and other loci is associated with the toxicity of the USA300 MRSA lineage.** Having
116 previously identified toxicity-associated, epistatic interactions occurring between the
117 mupirocin resistance (mup^R) conferring mutation in the *ileS* gene (G1762T) and other
118 loci within a collection of ST239 MRSA isolates[21], we sought to determine whether

119 this was lineage specific. We analysed toxicity and sequence data for a collection of
120 130 USA300 MRSA isolates[22], where the SNP conferring mup^R resistance emerged for
121 the USA300 isolates as the most dominant toxicity-affecting epistatically-interacting
122 locus (fig. 1), demonstrating the widespread nature of this effect across diverse
123 clonal lineages. See Supp. Table 1 for the list of loci associated with the mup^R
124 conferring SNP for both the ST239 and USA300 collections.
125 To illustrate the epistatic effect on toxicity we selected at random one of the
126 interacting loci and present the mean toxicity of the four combinations of each allele
127 of the two genes (Table 1). The SNP we selected was at position 480640 (relative to
128 the origin of replication) and confers a non-synonymous change in the protein
129 encoded by the open-reading frame with the locus tag SAUSA300_0426, which is
130 described as a conserved hypothetical protein. When in combination with the mup^R
131 encoding SNP in *ileS*, strains with the allele of SAUSA300_0426 containing a T at
132 position 480640 are significantly more toxic than those with a C at this site. Whereas
133 in the mupirocin sensitive strains, those with the C at position 480640 are more toxic
134 than those with a T at this site (Table 1). This example illustrates the toxicity
135 affecting epistatic signal detected by our analysis.
136
137 **Mupirocin resistance exerts a pleiotropic effect on the *S. aureus* proteome.**
138 Across both the ST239 and USA300 collections of isolates, 59 loci associated with the
139 toxicity of *S. aureus* through epistatic interactions with the mup^R mutation (Supp.
140 Table 1). To understand how such potential interactions could affect toxicity we
141 examined this list of loci, however, no known toxicity affecting genes were
142 identified, and no loci were common between the two clones. As IleRS is involved in
143 the translation of proteins, and our GWAS data suggests this antibiotic resistance
144 conferring mutation also affects the ability of *S. aureus* to secrete toxins, we
145 hypothesised that this mutation may have pleiotropic effects on protein production,
146 which could explain the observed epistasis. To examine this, we isolated a mup^R
147 version of the *S. aureus* laboratory strain SH1000 by plating overnight cultures on
148 agar containing 4μg/ml mupirocin. Mupirocin resistant colonies of the SH1000 strain
149 were recovered, and to confirm that the V588F conferring SNP was present the
150 colonies were sequenced and compared to SH1000. We selected a colony which we

151 have designated MY40, where the only non-synonymous SNP found in this strain
152 was that conferring the V588F change in IleRS, although a small number of non-
153 synonomous SNP differences were detected (Supp. Table 2).
154
155 We performed Tandem-Mass-Tagging (TMT) protein mass spectroscopy[23] on whole
156 cell lysates of the wild type SH1000 and mup^R strain MY40. The proteins were
157 extracted from triplicate 18hr cultures in Tryptone Soy Broth (TSB), and of the 3026
158 open reading frames predicted for the NCTC8325 chromosome (which is the closest
159 reference genome to SH1000), this proteomic approach was able to detect and
160 quantify 1284 proteins, where we used a cut-off of a minimum of a two-fold
161 difference in protein abundance to identify differentially produced proteins. When
162 we compared the proteome of SH1000 and MY40, there were 140 proteins that
163 were differentially produced (Supp. Table 3), which verified our hypothesis that this
164 resistance mutation has pleiotropic effects. However, when we compared this list of
165 differentially produced proteins with our list of loci associated with toxicity through
166 epistasis with the mup^R mutation (Supp. Table 1) there was no overlap, suggesting
167 any toxicity affecting interactions between these loci must be indirect.
168
169 **Exposure to mupirocin and mupirocin resistance have common effects on protein**
170 **production.** To examine whether the mup^R mutation has a similar effect on IleRS
171 activity as the presence of mupirocin has, alongside our proteomic analysis of the
172 the mup^R mutant we also analysed lysate of SH1000 exposed to the highest
173 concentrations of mupirocin for which we found no inhibition of growth (10ng/ml).
174 This concentration was selected to avoid any confounding effects differences in
175 growth rates might have on the proteome. Exposure of the wild type SH1000 strain
176 to mupirocin resulted in differential production of 67 proteins when compared to
177 the untreated SH1000 (Supp. Table 4), 18 of which were also different in the mup^R
178 mutant, suggesting many common down-steam effects of interfering with the
179 activity of IleRS. These include an increase in the production of several of the
180 proteins involved in Ile biosynthesis (i.e. LeuA, LeuC and IlvA), which suggests that
181 the bacteria are compensating for the interference in IleRS activity due to the
182 mutation and exposure to the antibiotic. Another common expression difference

183 was that several of the iron-regulated surface determinant (Isd) proteins were
184 expressed at lower levels in both the mutant and the mupirocin-exposed wild type
185 when compared with the untreated wild type. As yet we have no explanation for this
186 observation.
187
188 **Effect of mupirocin resistance on virulence regulating proteins.** The first virulence
189 related protein abundance difference between the SH1000 and its mup^R mutant we
190 noted was the AgrA protein[24]. This is the cytoplasmic response regulator of the Agr
191 toxicity regulating system which was produced at significantly higher levels in the
192 mutant (7-fold, Supp. Table 3). The *agrA* and *agrC* genes are co-transcribed,
193 however, there was no difference in AgrC protein abundance across the protein
194 preparations, which suggests that the effect on AgrA abundance must be post-
195 transcriptional. The AgrA protein needs to be phosphorylated to become
196 transcriptionally active, as such, were it active we would expect to see increased
197 transcription of the RNAIII effector molecule of the Agr system. To test this we
198 performed qRT-PCR on mRNA extracted from both the SH1000 and mup^R mutant,
199 where we found no difference in RNAIII expression (n=6, two-tailed t-test, p=0.49),
200 which suggests that although AgrA may be more abundant in the mutant it does not
201 seem to be transcriptionally active.
202
203 Other known virulence regulators were also identified as being differentially
204 produced in the mupirocin resistant strain. Both the SrrB and SarR proteins[24] were
205 expressed at higher levels in the mutant, whereas the Rot protein[24] was expressed at
206 lower levels compared to the wild type strains. Three other known regulatory
207 proteins were also differentially expressed (i.e. a GntR family transcriptional
208 regulator, the lytic regulatory protein SAOUHSC_02390, and the Pur operon
209 regulator, PurR), which when considered alongside the effect on the three virulence
210 regulators suggests that mupirocin resistance results in a significant re-wiring of *S.*
211 *aureus* regulatory processes.
212
213 **Effect of mupirocin resistance on toxin production.** Of the toxins encoded on the
214 SH1000 genome, there was significantly more of both delta toxin and PSMα1 in the

215 lysate of mupirocin resistant mutant (32- and 21-fold respectively, Supp. Table 3).
216 These are two of the most abundantly produced members of the Phenol Soluble
217 Modulin (PSM) family of cytolytic toxins[25]. As our original GWAS analysis was
218 focused on toxicity, we hypothesised that these differences may explain the
219 association we observed, and it suggests that the mutant should be more toxic than
220 the wild type strain. To test this we quantified the cytolytic activity of the wild type
221 and mutant by incubating bacterial supernatant with cultured THP-1 cells, which are
222 sensitive to the majority of cytolytic toxins produced by *S. aureus*, including the
223 PSMs[22]. While we found that mupirocin resistance did influenced toxicity, the effect
224 was the opposite to what our proteomic analysis suggested it should be, in that the
225 mupirocin resistant MY40 strain killed only 71% of the cells compared to the wild
226 type mupirocin sensitive SH1000 strain which killed 87% of the cells (n=6, two tailed
227 t-test; p=0.023). As our toxicity assays uses bacterial supernatant, whereas our
228 proteomic analysis was on whole cell lysates, it is possible that the difference in
229 abundance of the toxins is not equivalent between the intra- and extra- cellular
230 environments. To examine this we quantified the abundance of PSMs in the bacterial
231 supernatants where we found the PSMs to be 3.4-fold less abundant in the
232 supernatant of the mup^R mutant (n=6, two tailed t-test; p=0.001, a representative
233 image of is presented in fig. 2a), which explains our cytolytic results.
234
235 **Mupirocin resistance affects the activity of the PSM secretory apparatus, Pmt.** As
236 the PSMs are more abundant in the intracellular environment of the mup^R mutant,
237 but less abundant in the extracellular environment, we hypothesised that PSM
238 secretion may be affected in the mutant. This is facilitated by the activity of the PSM
239 export system, Pmt[26], and although the *pmt* genes have not been annotated on the
240 NCTC8325 genome, they are present (locus tags SAOUHSC_02155, SAOUHSC_02154,
241 SAOUHSC_02153, SAOUHSC_02152, SAOUHSC_02151). The locus encodes a
242 regulatory protein, two membrane bound ABC transporter proteins and two ATP
243 binding proteins that fuel the export system, where the four structural genes are
244 transcribed from a single promoter. Each ATP binding protein interacts with its
245 paired transporter protein and the maintained selection of the 1:1:1:1 stoichiometry
246 suggests it is critical to the exporters activity. In our mup^R mutant we found that

247 there was more than twice as much of one of the two ATP binding proteins
248 (SAOUHSC_02152, gene name *pmtC*) compared with the wild type strain. We
249 hypothesised that interference with the stoichiometry of the proteins in this export
250 system may explain why we have more PSM inside the cell but less outside. To test
251 this we cloned and expressed the *pmtC* gene, from an inducible promoter in the
252 SH1000 wild type background, and found that there was 2.8-fold less PSMs in the
253 extracellular environment when this ATPase was overexpressed (n=6, two tailed t-
254 test; p=0.003, a representative image of is presented in fig. 2b). This suggests that
255 the effect mupirocin resistance has on *S. aureus* toxicity is mediated by interfering
256 with the activity of the PSM secretory apparatus. It is interesting to consider that the
257 complete inactivation of the Pmt system has been shown to be lethal to the bacteria,
258 presumably as a result of the damage the PSMs can cause to internal membrane
259 structures[26]. While we demonstrate a partial blocking of the Pmt system by
260 mupirocin resistance, and some accumulation of PSMs internally, it must be a sub-
261 toxic level, as we see no *in vitro* growth defects associated with this.
262
263 **Reducing the production of toxins alleviates the fitness cost of mup^R**. With one
264 consequence of the significant changes mup^R causes to the proteome of *S. aureus*
265 being a reduction in toxin production, and with toxin production and secretion being
266 an energetically costly activity, we hypothesized that the down regulatory effect of
267 mupirocin resistance on toxin production may mask or alleviate the resistance
268 related fitness costs that are incurred. To test this we quantified the relative fitness[27]
269 of the mup^S and mup^R strains by competition in two genetic backgrounds; one in the
270 SH1000 wild-type background (i.e. SH1000 and MY40) where the bacteria can
271 express toxins. For the other, we inactivated the Agr quorum sensing system in both
272 SH1000 and MY40 by transducing in the inactivated Agr system (an erythromycin
273 resistance has been inserted into it) from the strain ROJ48[28], resulting in strains
274 MY18 and MY41. As reported previously, in the wild type background with a
275 functional Agr system, there was no difference in fitness between the mup^S SH1000
276 and the mup^R MY40 strains (fig. 3A; n=10; two-tailed t-test p=0.6). However, when
277 we quantified the relative fitness in the Agr defective background where neither
278 strain could produce toxins, such that any alleviation of fitness costs that result from

279 the relative reduction in toxicity of the mup^{R} mutant was nullified, we found the
280 fitness of the mup^{R} MY41 strain to be significantly lower than the mup^{S} MY18 strain
281 (fig. 3A; n=10; two-tailed t-test p=0.04). This demonstrates that this mupirocin
282 resistance conferring mutation does incur a fitness cost, but this cost can be masked
283 by reducing the costly production of toxins.
284
285 As the ability to produce toxins is selected for in environments such as the nose[29],
286 we hypothesised that in such an environment, the costs associated with this
287 resistance mechanism should become apparent, without having to genetically
288 manipulate the Agr system. To test this we developed a growth media with very low
289 levels of nutrients (0.1X TSB) but added 5% horse blood such that strains that can
290 produce toxins can release and utilise further nutrients from these blood cells for
291 growth. To avoid the less toxic cells benefiting from nutrients the more toxic cells
292 release, we quantified the growth rate of SH1000 and its mup^{R} mutant separately,
293 quantifying their Malthusians parameters at 3, 6 and 24hours in this medium. After
294 3hr of incubation in the medium there was no detectable growth of either strain,
295 however, by 6hrs both bacterial strains had grown, although the mup^{R} strain was
296 significantly more fit than the SH1000 strain (fig. 3B; n=6; two-tailed t-test p=0.007).
297 This suggests the bacteria enter a long lag phase in this medium, but once adapted
298 (after 3hrs) there was sufficient nutrients available to sustain some growth, with the
299 SH1000 strain at an apparent disadvantage, presumably by expending energy on
300 producing more toxins than its mup^{R} mutant. After the 6hr time-point there was a
301 distinct shift in the relative fitness of the strains, with the SH1000 strain becoming
302 relatively more fit than the mup^{R} strain (fig. 3B; n=6; two-tailed t-test p=0.04). The
303 increased relative growth rate of the wild type SH1000 strain is presumably as a
304 result of its increased capability to lyse cells and release nutrients necessary for its
305 growth. While the relative fitness of any organism is dependent upon its
306 environment, here we demonstrate how readily this can fluctuate within an
307 environment. That the fitness consequences of mupirocin resistance became
308 apparent when cell lysis became necessary may provide an explanation for why,
309 despite the ease at which this mutation can occur, it is not more prevalent and is
310 readily lost within healthy communities[20].

311

312 **The mup^R mutation has differing effects on toxicity in different *S. aureus***
313 **backgrounds.** Our proteomic analysis did not provide any evidence in support of a
314 direct interaction occurring between the mup^R *ileS* gene and the loci our GWAS
315 analysis has identified as interacting with this locus to affect toxicity (fig. 1 and Supp.
316 Table 1). As GWAS in bacteria can be confounded by population structures and
317 linkage disequilibrium, it is therefore possible that these polymorphic loci are instead
318 reflective of the genetic backgrounds of the bacteria that are sensitive to the effect
319 of the mup^R mutation to varying degrees. If true, then the introduction of the mup^R
320 mutation into different *S. aureus* strains should have differing effects on toxicity. To
321 test this we isolated mup^R colonies of two temporally and geographically diverse
322 isolates from the same clone as SH1000 (ST8 as determined by MLST), in the
323 laboratory strain RN6390B and in the USA300 clinical isolate USFL34. The presence
324 of the V588F mutation was confirmed by sequencing and the effect of the mutation
325 on toxicity quantified. Despite reducing the toxicity of the SH1000 background strain,
326 the mup^R mutation had no effect on toxicity in either RN6390B or USFL34 (n=6; two-
327 tailed t-test p=0.59 and 0.12 respectively), supporting our hypothesis that strains
328 respond differently to this antibiotic resistant mechanism, and providing an
329 explanation for our epistasis findings.
330

331 **CONCLUSION**

332 Understanding the evolution of antibiotic resistance, both in terms of how it
333 emerges and how it becomes stably maintained, is critical if identifying means of
334 curtailing its further emergence are to be developed. With some antibiotic resistance
335 mechanisms being reported as incurring no fitness costs[4-6], and others where
336 physiological and regulatory compensation of costs have been demonstrated[30-32], it
337 is perhaps surprising that they have not become more prevalent. Here, by adopting a
338 population-based functional genomics approach, we uncover hidden fitness costs
339 associated with an apparently cost-free, antibiotic resistance mechanism. We
340 demonstrate that the mupirocin-resistance conferring mutation of the gene
341 encoding the IleRS enzyme has pleiotropic effects on bacteria, which in hindsight is
342 perhaps unsurprising given the highly conserved and essential nature of this gene. In

343 this instance, while reducing the energetic expense associated with toxin production
344 provides a relief of the resistance-associated fitness costs, this appears to be
345 unsustainable when the ability to produce toxins is required. Given that the nose of
346 healthy carriers has been shown to be such a toxicity-dependent environment for *S.*
347 *aureus*, this toxicity related fitness off-setting may explain why this resistance
348 mechanism is not more prevalent, and is readily displaced, once this antibiotic has
349 been removed from their environment. An effect we would have been unable to
350 explain had we not adopted a population-based approach to studying this major
351 bacterial pathogen.
352
353

354 **MATERIALS AND METHODS**

355 **Strains and growth conditions**

356 All strains used in this study are listed in Supp. Table 5. *S. aureus* strains were grown
357 at 37°C, in either tryptic soy agar or broth (TSA/TSB) with the appropriate antibiotic
358 where necessary. The *E. coli* TOP10 strain containing the pAgrC(his)A plasmid was
359 grown in Luria-Bertani (LB) media with 100µg/ml ampicillin. THP-1 cells were grown
360 in RPMI 1640 supplemented with foetal bovine serum (10%), L-glutamine (2mM),
361 penicillin (100 units/ml) and streptomycin (100µg/ml) and incubated at 37°C with 5%
362 CO_2.

363

364 **Selection of the mupirocin resistant strain.**

365 As an essential gene *ileS* cannot be inactivated, and as a consequence, a homologous
366 recombination based mutational approach were unsuccessful. Therefore, to
367 generate isogenic mupirocin resistant and sensitive strains we utilised a selection
368 based method where an overnight culture of a mupirocin sensitive strain (e.g
369 SH1000 was plated onto agar plates with 4µg/ml mupirocin. This was incubated at
370 37°C for 48 hr and colonies that grew were further isolated by streaking onto fresh
371 mupirocin plates.

372

373 **Genome sequencing of the mup^{R} strain.**

374 *S. aureus* strain MY40 was sequenced in this study; DNA was extracted using the
375 QIAamp DNA Mini Kit (QIAGEN, Crawley, UK), using manufacturer's instructions with
376 1.5 µg/µL lysostaphin (Ambi Products LLC, NY, USA) to facilitate cell lysis. DNA was
377 quantified using a Nanodrop spectrophotometer, as well as the Quant-iT DNA Assay
378 Kit (Life Technologies, Paisley, UK) before sequencing. High-throughput genome
379 sequencing was performed using a MiSeq machine (Illumina, San Diego, CA, USA)
380 and the short read, paired-end data was assembled using the *de novo* assembly
381 algorithm SPAdes (Bankevich et al (SPADES). Sequence data are archived in the NCBI
382 repositories: GenBank Accession: SUB2754769, Short Read Archive (SRA):
383 SRR5651527, associated with BioProject: PRJNA384009. Assembled genomes are
384 also available on FigShare (doi.org/10.6084/m9.figshare.5089939.v1).

385

386 **Toxicity assays**

387 THP-1 cells[33] were grown as described above and harvested by centrifugation and
388 washed in PBS and diluted to a final density (determined by haemocytometer) of
389 $2x10^6$ cells per ml of PBS. Bacterial supernatant was harvested after 18hrs of growth
390 in TSB at 37°C. 20µl of the bacterial supernatant was mixed with 20µl of THP-1 cells,
391 and incubated for 12 mins at 37°C. 260µl of Guava ViaCount (Milipore) was added to
392 the sample, and incubated at room temperature for 5 mins before analysing the
393 viability on the Guava flow cytometer (Milipore).

394

395 **Fitness assays**.

396 The strains were cultured individually overnight and diluted to 10^4 cfu/ml. For the
397 direct competitions 25µl of each diluted culture was added into 5ml fresh TSB, and
398 grown at 37°C with shaking for 24h. The mixed culture was diluted and plated onto
399 agar plates with and without 4µg/ml mupirocin and incubated at 37°C. The resulting
400 colonies were counted, and the number of colonies from the mupirocin plate was
401 subtracted from the count from no antibiotic plate. The Malthusian parameter was
402 calculated using the following formula:

403 *Ln (final density (colony forming units (CFU)/ml) / starting density (CFU/ml))*

404 The Malthusian parameters of the mup^S and mup^R strains were compared using a
405 two tailed t-test. For the individual fitness assays the strains were cultured
406 individually overnight and diluted and added to 0.1X TSB made with phosphate
407 buffered saline rather than water to maintain the integrity of the horse blood cells to
408 which and 5% horse blood (Oxoid) was added. Bacterial growth was determined by
409 plating the cultures on TSA plates after 3, 6 and 24hrs of incubation at 37°C in air.

410

411 **Deletion of the *agr* locus from SH1000 and MY40.**

412 Phage transduction was used to construct the mup^R and mup^S Agr mutants. In the *S.*
413 *aureus* strain ROJ48, the entire Agr locus has been replaced with an erythromycin
414 resistance cassette[28]. This was moved from ROJ48 into SH1000 by phage
415 transduction as follows: ROJ48 φ11 lysates were prepared from 200µl of overnight
416 ROJ48 culture in LK (1% Tryptone, 0.5% yeast extract, 1.6% KCl) which was added to
417 3ml of fresh LK and 3ml of phage buffer (10mM $MgSO_4$, 4mM $CaCl_2$, 50mM Tris-HCl

418 pH 7.8, 100mM NaCl and 0.1% gelatine powder in molecular/MiliQ water), and to
419 this 500µl φ11-RN6390B lysate was added. This was incubated at 30°C shaking until
420 the media became clear, which indicated bacterial lysis. The lysates were then filter
421 sterilised, and a second round of lysis was carried out on ROJ48 with this first round
422 lysate. After these two lysis steps, transduction into SH1000 and MY40 strains was
423 performed by adding 200µl of overnight culture to 1.8ml LK with 10µl 1M $CaCl_2$, and
424 500µl the φ11-ROJ48 lysate. This was incubated at 37°C with shaking for 45 min,
425 then 1ml ice cold 20mM trisodium citrate was added and the transducing mixture
426 was placed on ice for 5 min. The bacteria were harvested by centrifugation and re-
427 suspended with 1ml ice cold 20mM trisodium citrate. This was incubated on ice for
428 2.5h, and plated onto TSA plates with 20mM trisodium citrate, erythromycin and
429 lincomycin (25µg/ml) which was incubated overnight at 37°C.
430
431 **qRT-PCR**
432 Overnight cultures of were diluted 1:500 into 3ml fresh TSB-chloramphenicol. After
433 18hr of growth 2 ml of this culture was mixed with 4ml RNA Protect Bacteria
434 (Qiagen), and the RNeasy Mini Kit (Qiagen) was used to extract RNA following the
435 manufacturer's protocol. Lysostaphin (200µg/ml) was added to Tris-EDTA buffer
436 (Ambion), and this was added to the sample after the RNA Protect step before
437 continuing with the protocol. When the RNA was extracted, Turbo DNA-free kit
438 (Thermo) was used to remove genomic DNA from the RNA samples; 3µl Turbo DNase
439 was added to the sample and incubated for 1.5h at 37°C, the a further 4µl Turbo
440 DNase was added and incubated for 1.5h. 35µl DNase inactivation reagent was
441 added to the samples to inactivate the DNase according to the protocol. The
442 concentration of RNA in the samples were measured using Qubit RNA Broad Range
443 kit (Thermo) and normalised before using QuantiTect Reverse Transcription Kit
444 (Qiagen) to convert the RNA samples into cDNA according to the manufacturer's
445 protocol. After adding the reverse transcriptase, the samples were incubated at 42°C
446 for 20 min before raising the temperature to 95°C for 3 mins to inactivate the
447 reverse transcriptase. Primers for *gyrB*, a housekeeping gene, was used alongside
448 those for RNAIII to standardise transcript levels (gyrB forward:
449 CCAGGTAAATTAGCCGATTGC, gyrB reverse: AAATCGCCTGCGTTCTAGAG. RNAIII

450 forward; AGCATGTAAGCTATCGTAAACAAC, RNAIII reverse;
451 TTCAATCTATTTTTGGGGATG). ssoAdvanced SYBR Green Supermix (Bio-Rad) was
452 used, using a standard curve of known genomic DNA concentrations for each primer
453 set. 5µl of samples, standards and water were pipetted into the wells of a 96-well
454 PCR plate. The supermix was added to water and primers according to the
455 manufacturer's protocol, and 15µl of this mix was pipetted over the DNA samples.
456 This was then placed into a qPCR machine, and run using the manufacturer's
457 recommendation. The quantity of RNA III cDNA was divided by the quantity of *gyrB*
458 cDNA to get a ratio of RNAIII transcription levels.
459
460 **PSM quantification in supernatants.**
461 An overnight culture of SH1000 and MY40 was diluted 1:1000 into 50ml fresh TSB,
462 and grown for 18h. The cultures were centrifuged at 18,000 rpm for 10 min, and
463 35ml of the supernatant was mixed with 10ml butanol. The samples were incubated
464 at 37°C shaking for 3h, and were then centrifuged at 3,000 rpm for 3 min and 1ml of
465 the upper organic layer was taken off. The samples were then freeze-dried overnight
466 and then re-suspended in 160µl 8M urea, separated on an SDS-PAGE gel and PSMs
467 quantified by densitometry analysis using the ImageJ software.
468
469 **TMT Labelling and High pH reversed-phase chromatography**
470 Aliquots of 100µg of up to ten samples per experiment were digested with trypsin
471 (2.5µg trypsin per 100µg protein; 37°C, overnight), labelled with Tandem Mass Tag
472 (TMT) ten plex reagents according to the manufacturer's protocol (Thermo Fisher
473 Scientific,) and the labelled samples pooled. An aliquot of the pooled sample was
474 evaporated to dryness and resuspended in buffer A (20 mM ammonium hydroxide,
475 pH 10) prior to fractionation by high pH reversed-phase chromatography using an
476 Ultimate 3000 liquid chromatography system (Thermo Fisher Scientific). In brief, the
477 sample was loaded onto an XBridge BEH C18 Column (130Å, 3.5 µm, 2.1 mm X 150
478 mm, Waters, UK) in buffer A and peptides eluted with an increasing gradient of
479 buffer B (20 mM Ammonium Hydroxide in acetonitrile, pH 10) from 0-95% over 60
480 minutes. The resulting fractions were evaporated to dryness and resuspended in 1%

481 formic acid prior to analysis by nano-LC MSMS using an Orbitrap Fusion Tribrid mass
482 spectrometer (Thermo Scientific).
483
484 **Nano-LC Mass Spectrometry**
485 High pH RP fractions were further fractionated using an Ultimate 3000 nanoHPLC
486 system in line with an Orbitrap Fusion Tribrid mass spectrometer (Thermo Scientific).
487 In brief, peptides in 1% (vol/vol) formic acid were injected onto an Acclaim PepMap
488 C18 nano-trap column (Thermo Scientific). After washing with 0.5% (vol/vol)
489 acetonitrile 0.1% (vol/vol) formic acid peptides were resolved on a 250 mm × 75 µm
490 Acclaim PepMap C18 reverse phase analytical column (Thermo Scientific) over a 150
491 min organic gradient, using 7 gradient segments (1-6% solvent B over 1min., 6-15%
492 B over 58min., 15-32%B over 58min., 32-40%B over 5min., 40-90%B over 1min., held
493 at 90%B for 6min and then reduced to 1%B over 1min.) with a flow rate of 300 nl
494 min^{-1}. Solvent A was 0.1% formic acid and Solvent B was aqueous 80% acetonitrile
495 in 0.1% formic acid. Peptides were ionized by nano-electrospray ionization at 2.0kV
496 using a stainless steel emitter with an internal diameter of 30 µm (Thermo Scientific)
497 and a capillary temperature of 275°C.
498 All spectra were acquired using an Orbitrap Fusion Tribrid mass spectrometer
499 controlled by Xcalibur 2.0 software (Thermo Scientific) and operated in data-
500 dependent acquisition mode using an SPS-MS3 workflow. FTMS1 spectra were
501 collected at a resolution of 120 000, with an automatic gain control (AGC) target of
502 200 000 and a max injection time of 50ms. Precursors were filtered with an intensity
503 threshold of 5000, according to charge state (to include charge states 2-7) and with
504 monoisotopic precursor selection. Previously interrogated precursors were excluded
505 using a dynamic window (60s +/-10ppm). The MS2 precursors were isolated with a
506 quadrupole mass filter set to a width of 1.2m/z. ITMS2 spectra were collected with
507 an AGC target of 10 000, max injection time of 70ms and CID collision energy of 35%.
508 For FTMS3 analysis, the Orbitrap was operated at 50 000 resolution with an AGC
509 target of 50 000 and a max injection time of 105ms. Precursors were fragmented by
510 high energy collision dissociation (HCD) at a normalised collision energy of 60% to
511 ensure maximal TMT reporter ion yield. Synchronous Precursor Selection (SPS) was
512 enabled to include up to 5 MS2 fragment ions in the FTMS3 scan.

513

514 **Proteomic data analysis**

515 The raw data files were processed and quantified using Proteome Discoverer
516 software v2.1 (Thermo Scientific) and searched against the UniProt Staphylococcus
517 aureus strain NCTC 8325 database using the SEQUEST algorithm. Peptide precursor
518 mass tolerance was set at 10ppm, and MS/MS tolerance was set at 0.6Da. Search
519 criteria included oxidation of methionine (+15.9949) as a variable modification and
520 carbamidomethylation of cysteine (+57.0214) and the addition of the TMT mass tag
521 (+229.163) to peptide N-termini and lysine as fixed modifications. Searches were
522 performed with full tryptic digestion and a maximum of 2 missed cleavages were
523 allowed. The reverse database search option was enabled and all peptide data was
524 filtered to satisfy false discovery rate (FDR) of 5%.

525

526

527 **REFERENCES**

528 1. Moura de Sousa, J., Balbontín, R., Durão, P. & Gordo, I. Multidrug-resistant
529 bacteria compensate for the epistasis between resistances. PLOS Biol. 15, e2001741
530 (2017).
531 2. Tenover, F. C. Mechanisms of Antimicrobial Resistance in Bacteria. Am. J.
532 Med. 119, S3–S10 (2006).
533 3. Levin, B. R., Perrot, V. & Walker, N. Compensatory mutations, antibiotic
534 resistance and the population genetics of adaptive evolution in bacteria. Genetics
535 154, 985–997 (2000).
536 4. Hurdle, J. G., O'Neil, A. J. & Chopra, I. The isoleucyl-tRNA synthetase mutation
537 V588F conferring mupirocin resistance in glycopeptide-intermediate Staphylococcus
538 aureus is not associated with a significant fitness burden. J. Antimicrob. Chemother.
539 53, 102–104 (2003).
540 5. Stanczak-Mrozek, K. I. et al. Within-host diversity of MRSA antimicrobial
541 resistances. J. Antimicrob. Chemother. 70, 2191–2198 (2015).
542 6. Knight, G. M., Budd, E. L. & Lindsay, J. A. Large mobile genetic elements
543 carrying resistance genes that do not confer a fitness burden in healthcare-
544 associated meticillin-resistant Staphylococcus aureus. Microbiol. (United Kingdom)
545 159, 1661–1672 (2013).
546 7. Rasigade, J.-P. & Vandenesch, F. Staphylococcus aureus: a pathogen with still
547 unresolved issues. Infect. Genet. Evol. 21, 510–4 (2014).
548 8. Lowy, F. Antimicrobial resistance: the example of Staphylococcus aureus. J.
549 Clin. Invest. 111, 1265–1273 (2003).
550 9. Wertheim, H. F. et al. The role of nasal carriage in Staphylococcus aureus
551 infections. Lancet Infect. Dis. 5, 751–762 (2005).
552 10. Gordon, R. J. & Lowy, F. D. Pathogenesis of Methicillin‐Resistant
553 Staphylococcus aureus Infection. Clin. Infect. Dis. 46, S350‐S359 (2008).

554 11. Abad, C. L., Pulia, M. S. & Safdar, N. Does the Nose Know? An Update on
555 MRSA Decolonization Strategies. Curr. Infect. Dis. Rep. 15, 455–464 (2013).
556 12. Thomas, C. M., Hothersall, J., Willis, C. L. & Simpson, T. J. Resistance to and
557 synthesis of the antibiotic mupirocin. Nat. Rev. Microbiol. 8, 281–289 (2010).
558 13. Simor, A. E. Staphylococcal decolonisation: An effective strategy for
559 prevention of infection? Lancet Infect. Dis. 11, 952–962 (2011).
560 14. Bertino Jr, J. S. Intranasal mupirocin for outbreaks of methicillin- resistant
561 Staphylococcus aureus. Am J Heal. Pharm 54, 2185–2191 (1997).
562 15. Antonio, M., McFerran, N. & Pallen, M. J. Mutations affecting the Rossman
563 fold of isoleucyl-tRNA synthetase are correlated with low-level mupirocin resistance
564 in Staphylococcus aureus. Antimicrob. Agents Chemother. 46, 438–442 (2002).
565 16. Patel, J. B., Gorwitz, R. J. & Jernigan, J. A. Mupirocin Resistance. Clin. Infect.
566 Dis. 49, 935–941 (2009).
567 17. Udo, E. E. & Sarkhoo, E. Genetic analysis of high-level mupirocin resistance in
568 the ST80 clone of community-associated meticillin-resistant Staphylococcus aureus.
569 J. Med. Microbiol. 59, 193–199 (2010).
570 18. Seah, C. et al. MupB, a New High-Level Mupirocin Resistance Mechanism in
571 Staphylococcus aureus. Antimicrob. Agents Chemother. 56, 1916–1920 (2012).
572 19. Hetem, D. J. & Bonten, M. J. M. Clinical relevance of mupirocin resistance in
573 Staphylococcus aureus. J. Hosp. Infect. 85, 249–256 (2013).
574 20. Williamson D.A., Carter G.P. & Howden B.P. Current and Emerging Topical
575 Antibacterials and Antiseptics: Agents, Action, and Resistance Patterns. Clin.
576 Microbiol. Rev. 30, 827-860 (2017).
577 21. Laabei, M. et al. Predicting the virulence of MRSA from its genome sequence.
578 Genome Res. 24, 839–849 (2014).
579 22. Laabei et al. Evolutionary Trade-Offs Underlie the Multi-faceted Virulence of
580 Staphylococcus aureus. PLoS Biol. 13(9):e1002229 (2015).
581 23. Dayon L & JC Sanchez. Relative protein quantification by MS/MS using the
582 tandem mass tag technology. Methods Mol Biol. 893:115-27 (2012).
583 24. Bronner, S., Monteil, H. & Prévost, G. Regulation of virulence determinants in
584 Staphylococcus aureus : complexity and applications. FEMS Microbiol. Rev. 28, 183–
585 200 (2004).
586 25. Qi, R. et al. Increased In Vitro Phenol-Soluble Modulin Production is
587 Associated with Soft Tissue Infection Source in Clinical Isolates of Methicillin-
588 Susceptible Staphylococcus aureus. J. Infect. 72, 302–308 (2017).
589 26. Chatterjee, S. S. et al. Essential Staphylococcus aureus toxin export system.
590 Nat. Med. 19, 364–367 (2013).
591 27. Lenski, R. E., Rose, M. R., Simpson, S. C. & Tadler, S. C. Long-Term
592 Experimental Evolution in Escherichia coli. I. Adaptation and Divergence During
593 2,000 Generations. Am. Nat. 138, 1315–1341 (1991).
594 28. Jensen, R. O., Winzer, K., Clarke, S. R., Chan, W. C. & Williams, P. Differential
595 Recognition of Staphylococcus aureus Quorum-Sensing Signals Depends on Both
596 Extracellular Loops 1 and 2 of the Transmembrane Sensor AgrC. J. Mol. Biol. 381,
597 300–309 (2008).
598 29. Recker M, et al. Clonal differences in Staphylococcus aureus bacteraemia-
599 associated mortality. Nat Microbiol. 2, 1381-1388 (2017).

600 30. Pacheco, JO, Alvarez-Ortega, C, Rico, MA & Martínez, JL. Metabolic
601 Compensation of Fitness Costs Is a General Outcome for Antibiotic-Resistant
602 Pseudomonas aeruginosa Mutants Overexpressing Efflux Pumps. mBio. 8, e00500-17
603 (2017).
604 31. Freihofer P, et al. Nonmutational compensation of the fitness cost of
605 antibiotic resistance in mycobacteria by overexpression of tlyA rRNA methylase.
606 RNA. 22, 1836-1843 (2016).
607 32. Collins, J et al. Offsetting virulence and antibiotic resistance costs by MRSA.
608 ISME J. 4, 577-84 (2010).
609 33. Tsuchiya, S. et al. Establishment and characterization of a human acute
610 monocytic leukemia cell line (THP‐1). Int. J. Cancer 26, 171‐176 (1980).
611
612
613
614

615
616 **FIGURES**

617

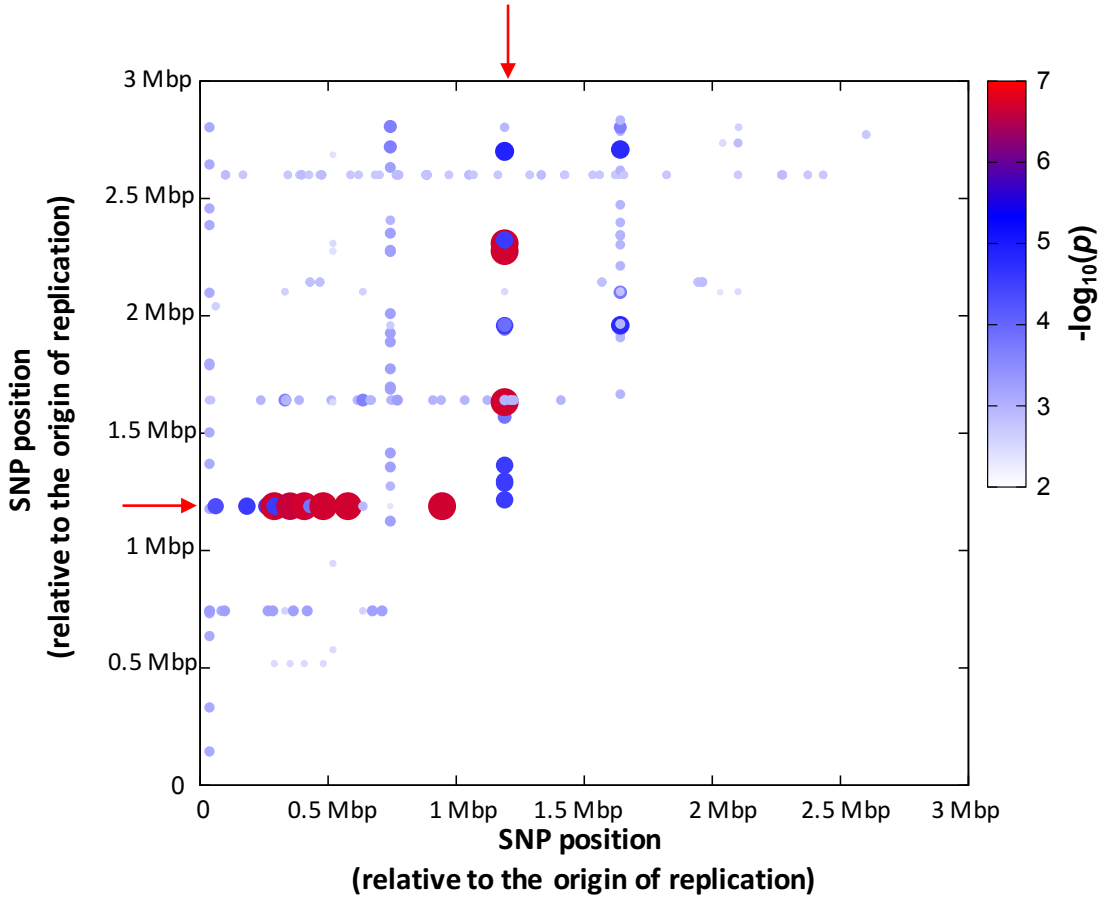

618

619 **Fig. 1:** Epistasis between the mupirocin resistance encoding mutation in the *ileS* gene
620 and many other loci is associated with the toxicity of the USA300 lineage of MRSA.
621 This heat map illustrates where specific combinations of the polymorphic site in the
622 *ileS* gene and polymorphic sites elsewhere on the chromosome are associated with
623 the toxicity of individual isolates. The mup^{R} conferring site is indicated on the X and Y
624 axis by the red arrow.

625

626

627

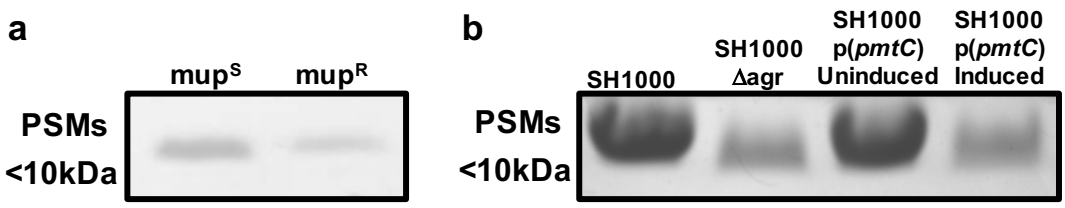

Fig. 2: PSM abundance in the *S. aureus* supernatant. The bacterial strains were grown in TSB for 18hrs. The PSMs were harvested from the bacterial supernatant by butanol extraction and run on an SDS-PAGE gel. **a**: There is significantly less PSM in the supernatant of the mupirocin resistant *S. aureus* strain compared to the wild type mupirocin sensitive strain. **b**: Over-expression of the *pmtC* gene, which encodes one of the ATP binding proteins of the PSM secretory system, Pmt, in the wild type SH1000 strain causes a reduction in the abundance of the PSM in the *S. aureus* supernatant. An Agr mutant has been provide as a control. A full length SDS-PAGE gel has been provided in Supplementary material (Supp. Fig. 1), to illustrate why we only provide a 'letter-box' snap-shot of the gels here.

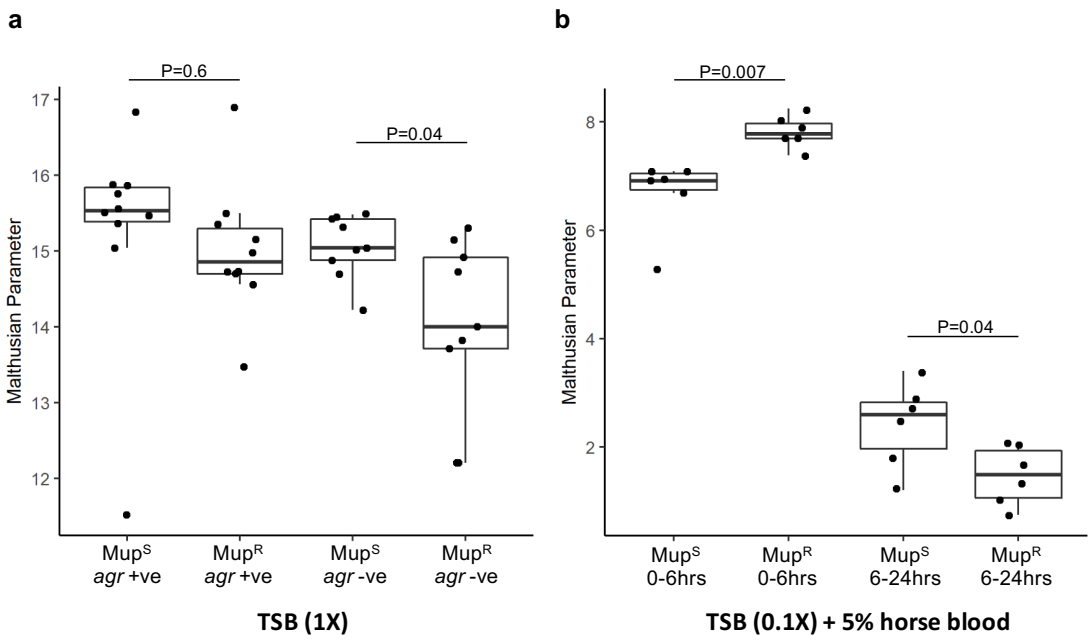

Fig. 3: Mupirocin resistance affect the relative fitness of *S. aureus.* **a**: the effect of mupirocin resistance on the relative fitness of *S. aureus* was determined in strains with and without a functioning Agr system by direct competition in TSB. There was no difference in fitness in the Agr +ve background, but in the absence of Agr, the mupirocin resistant strain was less fit that the mupirocin sensitive strain. **b**: The effect of mupirocin resistance on relative fitness was determined by individual culture in a nutrient poor environment (0.1X TSB) supplemented with 5% horse blood. At the early stages of growth (0-6hrs) the mupirocin sensitive strain was more fit, whereas between 6 and 24hr when the nutrients in the TSB were depleted and cell lysis became necessary, the mupirocin sensitive strains was relatively more fit.

656
657
658 **TABLES**

659 **Table 1:** Toxicity affecting epistatic interactions. An example of a SNP associated by
660 our epistasis analysis to be interacting with the mupirocin resistance conferring SNP
661 to affect toxicity. The mean toxicity of each of the four combinations of the four
662 alleles is presented +/- the 95% confidence intervals.

Percentage Cell death (+/- 95% confidence)	SAUSA300_0426 (T)	SAUSA300_0426 (C)
Mupirocin resistant	45.6% (+/- 5.7)	4.6% (+/- 2.8)
Mupirocin sensitive	20.65% (+/- 4)	53% (+/- 9.2)

663
664